Crystal structure of a substrate-free aspartate transporter

Jensen, Sonja; Guskov, Albert; Rempel, Stephan; Hänelt, Inga; Slotboom, Dirk

Published in:
Nature Structural & Molecular Biology

DOI:
10.1038/nsmb.2663

Publication date:
2013

Crystal structure of a substrate-free aspartate transporter

Sonja Jensen[1,3], Albert Guskov[1,3], Stephan Rempel[1], Inga Hänelt[1] & Dirk Jan Slotboom[1,2]

Archaeal glutamate transporter homologs catalyze the coupled uptake of aspartate and three sodium ions. After the delivery of the substrate and sodium ions to the cytoplasm, the empty binding site must reorient to the outward-facing conformation to reset the transporter. Here, we report a crystal structure of the substrate-free transporter Glt_{Tk} from *Thermococcus kodakarensis*, which provides insight into the mechanism of this essential step in the translocation cycle.

Glutamate transporters are secondary transporters found in many eukaryotes, bacteria and archaea[1]. In prokaryotes these transporters mediate the uptake of nutrients, whereas in mammals, where glutamate is a major excitatory neurotransmitter, they catalyze the neurotransmitter reuptake into neurons and glial cells that follows synaptic signal transduction. Maintaining a low extracellular concentration of the neurotransmitter is essential for sensitive signal transmission and for the prevention of neurotoxicity. The transporters couple the uptake of glutamate to the symport of cations: three sodium ions and one proton are co-transported by the neuronal and glial transporters[2]. After the substrate and cations are released into the cytoplasm, the empty binding site reorients to an outward-facing orientation. In mammalian transporters this reorientation is strictly coupled to the export of a potassium ion, but in prokaryotes no such coupling is required[3].

Structural information is available for the glutamate transporter homolog Glt_{Ph} from the archaeon *Pyrococcus horikoshii*, which is selective for aspartate rather than glutamate and which couples the uptake of substrate to the symport of three sodium ions[3–8]. The protein is a homotrimer, with each protomer consisting of two domains. The trimerization domain mediates the subunit contacts, and the transport domain carries the binding sites for aspartate and sodium ions. Different crystal structures of substrate-bound Glt_{Ph} have revealed that the trimerization domains form a stable scaffold[6,9]. The transport domains have been captured in three states: outward facing, intermediate and inward facing[5–7]. The structures suggest that the transport domains behave as rigid bodies and move across the membrane like an elevator to shuttle the substrate and coupled ions from one side to the other. Because the transporters are substrate loaded in all available crystal structures, the mechanism by which the empty (substrate-free) transporter reorients to the outward-facing position after delivery of the substrates to the cytoplasm remained elusive. To gain insight into this essential part of the transport cycle, we determined the structure of a substrate-free transporter.

We purified glutamate transporter homologs from several closely related Archaea, using a protocol that yields the protein devoid of aspartate and sodium ions[8] (see also Online Methods). The reason that we did not focus exclusively on Glt_{Ph} was to increase our chances of obtaining well-diffracting crystals. We obtained pure and stable preparations of Glt_{Tk} from the thermophilic archaeon *T. kodakarensis*. Glt_{Tk} shares 77% sequence identity with Glt_{Ph}, and all residues that interact with the substrate aspartate in Glt_{Ph} are strictly conserved in Glt_{Tk} (**Supplementary Fig. 1**). The residues that shape the two Na^+-binding sites found in the Glt_{Ph} crystal structures are also conserved. The location of the third Na^+-binding site is still debated[10–12]. The two transporters are functionally similar as well. Just like Glt_{Ph} (ref. 3), Glt_{Tk} is a sodium-coupled aspartate transporter that also accepts D-aspartate but not glutamate as substrate (**Supplementary Fig. 2**). Importantly, we confirmed by isothermal titration calorimetry that our preparations of Glt_{Tk} were free of Na^+ and aspartate (**Supplementary Fig. 3**).

We solved the structure of apo-Glt_{Tk} to a resolution of 3.0 Å (see **Supplementary Table 1** for data collection and refinement statistics). The extensive sequence similarity between Glt_{Ph} and Glt_{Tk}, as well as their functional resemblance, allowed for a comparison between the substrate-bound structures available for Glt_{Ph} and the structure of the apoprotein of Glt_{Tk}. The overall structure of Glt_{Tk} is very similar to that of Glt_{Ph}, with the transport domain in the outward-facing

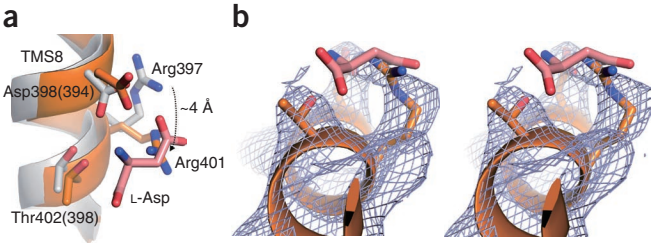

Figure 1 Aspartate-binding site. (**a**) Comparison of the aspartate-binding sites in Glt_{Ph} and Glt_{Tk}. Relevant amino acid residues are shown as sticks and labeled and numbered as in Glt_{Tk} (and as in Glt_{Ph} in parentheses). Glt_{Ph} is colored in gray, the substrate L-aspartate from Glt_{Ph} in light red and Glt_{Tk} in orange. The large shift of Arg401(397) in TMS 8 is indicated with an arrow. (**b**) Stereo image of the substrate-binding site of Glt_{Tk} with electron density ($2F_o - F_c$ map, contoured at 1.2σ). Glt_{Tk} is shown in orange, and the substrate L-aspartate present in Glt_{Ph} is shown in light red to emphasize the clash with the position of Arg401 in Glt_{Tk}.

[1]Groningen Biomolecular Sciences and Biotechnology Institute, University of Groningen, Groningen, The Netherlands. [2]Zernike Institute for Advanced Materials, University of Groningen, Groningen, The Netherlands. [3]These authors contributed equally to this work. Correspondence should be addressed to D.J.S. (d.j.slotboom@rug.nl).

Received 8 May; accepted 2 August; published online 8 September 2013; doi:10.1038/nsmb.2663

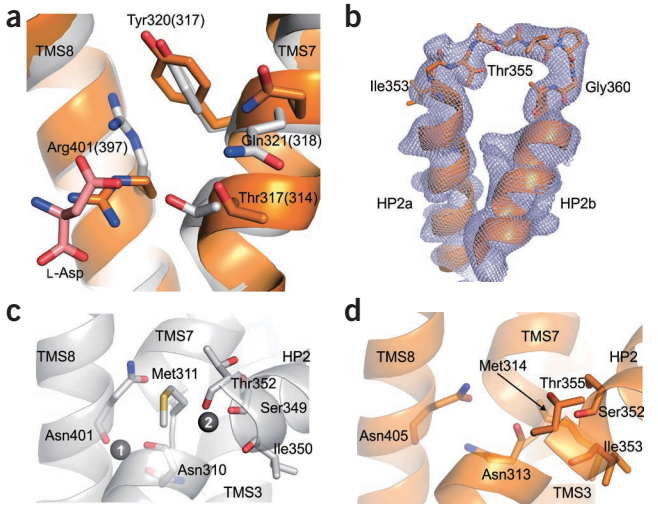

Figure 2 Cation-binding sites. (**a**) Overlay of Glt_{Tk}, in orange, with Glt_{Ph}, in gray (the substrate L-aspartate is shown in light red). The cation-π interaction between Arg397 and Tyr317 of Glt_{Ph} is disrupted in Glt_{Tk} and a cavity is created, which could form a potassium-binding site in the eukaryotic members of the glutamate transporter family. Numbering of residues is for Glt_{Tk}, with numbers for Glt_{Ph} in parentheses. (**b**) Electron density of HP2 ($2F_o - F_c$ map, contoured at 1.2σ). (**c**,**d**) Comparison of Na^+-binding sites of Glt_{Ph} (**c**, in gray) with Glt_{Tk} (**d**, in orange). The two Na^+-binding sites of Glt_{Ph} are indicated 1 and 2. Relevant residues are labeled and numbered according to the Glt_{Ph} or Glt_{Tk} sequence in **c** and **d**, respectively.

conformation (**Supplementary Fig. 4a**)[4,5]. The two helical hairpins (HP1 and HP2) in the transport domain, which may form intra- and extracellular gates, respectively, occlude the substrate-binding site in both Glt_{Ph} and Glt_{Tk} (**Supplementary Fig. 4b**).

Despite these similarities in global structure, there are crucial differences in the binding sites for aspartate and sodium ions. In the aspartate-binding site, Arg401 of Glt_{Tk} in transmembrane segment (TMS) 8 adopts a very different conformation from the equivalent Arg397 of Glt_{Ph} (**Fig. 1**). This arginine is highly conserved in the glutamate transporter family and is essential for transport[13–15]. Compared to that in Glt_{Ph}, the guanidium group of Arg401 in Glt_{Tk} is offset by ~4 Å, and its position overlaps that occupied by the substrate aspartate in Glt_{Ph}. Thus, in the empty carrier, the side chain of a highly conserved residue takes over the site occupied by the transported ligand in the loaded carrier. Because the overlap is not complete, we assume that water molecules fill up the rest of the empty binding site. The position of the guanidium group of Arg401 is stabilized by an ionic interaction with conserved Asp398 (394, where the numbering in parentheses is for Glt_{Ph}). In substrate-bound Glt_{Ph} this residue interacts with the amino group of the substrate aspartate (**Supplementary Fig. 5**). The side chain *B*-factors of Arg401 are slightly higher than the average in the protein (**Supplementary Table 2**); this could be related to the dynamic role of Arg401, which should be able to reposition during the translocation cycle.

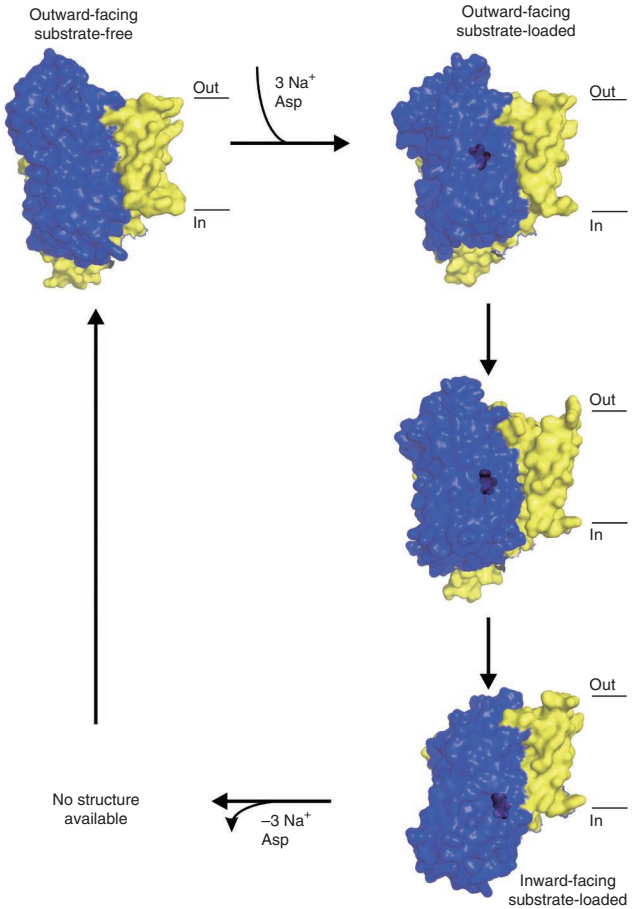

The repositioning of Arg401 has another consequence as it breaks the cation-π interaction with Tyr320 (317) in TMS7 that is present in substrate-bound Glt_{Ph} (ref. 4). This breakage allows for rearrangements in TMS7, notably of Tyr320 (317), Gln321 (318) and Thr317 (314) (**Fig. 2a**). In Glt_{Ph} the location of the latter residue is stabilized by a hydrogen bond with the α-carboxylate of the substrate aspartate, but in the substrate-free transporter it can reorient, which also affects the region around Met314(311) in TMS7 (see below). In the rat transporter GLT-1, the equivalents of Tyr320 and Gln321 (Tyr403 and Glu404, respectively) are essential for the coupling with potassium ions, which is required for reorientation of the empty carrier in mammalian glutamate transporters[16,17]. The rearrangement of residues around Arg401 in apo-Glt_{Tk} creates a pocket, which in the mammalian transporters may form a potassium-binding site (**Fig. 2a**). The structure provides an explanation for a key finding in the neuronal glutamate transporter EAAC1. When the equivalent of Arg401 (Arg447 in EAAC1) was mutated into cysteine, the protein could no longer bind or transport glutamate and aspartate, but it was still able to transport neutral amino acids. However, only exchange of the neutral amino acids could take place, and net transport was impaired, showing that the conserved arginine is crucial not only for the binding of acidic substrates but also for the reorientation of the empty carrier[15].

In both Glt_{Tk} and Glt_{Ph}, TMS7 is partially unwound in the center of the membrane. The unwound part in Glt_{Tk} has undergone a dramatic change of conformation around Met314, which is a highly conserved and functionally important residue[14,18]. The side chain of Met314 in the empty transporter points away from the binding site (**Fig. 2b–d**)

Figure 3 Translocation cycle of archaeal aspartate transporters based on the available crystal structures. Shown (clockwise from top right) are surface representations of a single subunit of the trimeric protein in the outward-facing substrate-loaded (PDB 2NWL)[5], intermediate substrate-loaded (PDB 3V8G)[7], inward-facing substrate-loaded (PDB 3KBC)[6] and outward-facing substrate-free (current structure) states. No structures are available for the inward-facing and intermediate states of the substrate-free transporters. The trimerization domain is in yellow, the transport domain in blue and the substrate L-aspartate in purple.

and is exposed to the lipid bilayer between Leu92 of TMS3 and Val349 of HP2. In Glt_{Ph} the side chain of the equivalent Met311 points toward the binding site and is located between the two sodium-binding sites that were found in the Glt_{Ph} crystal structures.

The change in conformation of the unwound part of TMS7 in Glt_{Tk} directly affects the first Na^+-binding site, as the backbone carbonyl oxygen of Asn313 (310) is displaced and is no longer in a favorable position to coordinate a sodium ion. Similarly, the carbonyl oxygen of Asn405 (401) in Glt_{Tk} is not properly oriented to bind the sodium ion. The second Na^+-binding site is also deformed in Glt_{Tk}. The backbone carbonyls of Ser352, Ile353 and Thr355 in HP2 that coordinate the second sodium ion in the Glt_{Ph} structure are displaced by 4 Å, 1.8 Å and 4.5 Å in Glt_{Tk}, thus impeding the binding of the cation (**Fig. 2b–d**).

The structure of apo-Glt_{Tk} provides an explanation for the mechanism of reorientation of the empty carrier. Because the overall structures of both the trimerization and the transport domains of the apoprotein are very similar to those of the corresponding domains in the substrate-loaded Glt_{Ph}, it is plausible that the movement of the transport domain across the membrane will take place in the empty carrier in the same manner as it does in the loaded carrier (**Fig. 3**). This hypothesis is supported by recent EPR experiments on Glt_{Ph}, which showed that the transport domain is structurally heterogeneous both in the apo and in the substrate-bound transporter, indicating a movement across the membrane in both conditions[19,20].

METHODS

Methods and any associated references are available in the online version of the paper.

Accession codes. Atomic coordinates and structure factors for the *Thermococcus kodakarensis* Glt_{Tk} transporter in its substrate-free state are deposited in the Protein Data Bank under accession code 4KY0.

Note: Any Supplementary Information and Source Data files are available in the online version of the paper.

ACKNOWLEDGMENTS

We thank B. Poolman and M. Jaehme for critically reading the manuscript and the European Synchrotron Radiation Facility for beamline access. This work was supported by the Deutsche Forschungsgemeinschaft (I.H.) (HA 6322/1-1), the Netherlands Organisation for Scientific Research (NWO vidi 700.54.423 and vici 865.11.001 grants to D.J.S.) and the European Union (EU EDICT program and European Research Council starting grant 282083 to D.J.S.).

AUTHOR CONTRIBUTIONS

All authors designed experiments. I.H. constructed the expression vector. S.J., A.G. and S.R. performed all other experiments. S.J., A.G., S.R. and D.J.S. analyzed data. S.J., A.G. and D.J.S. wrote the manuscript.

COMPETING FINANCIAL INTERESTS

The authors declare no competing financial interests.

1. Danbolt, N.C. *Prog. Neurobiol.* **65**, 1–105 (2001).
2. Zerangue, N. & Kavanaugh, M.P. *Nature* **383**, 634–637 (1996).
3. Ryan, R.M., Compton, E.L. & Mindell, J.A. *J. Biol. Chem.* **284**, 17540–17548 (2009).
4. Yernool, D., Boudker, O., Jin, Y. & Gouaux, E. *Nature* **431**, 811–818 (2004).
5. Boudker, O., Ryan, R.M., Yernool, D., Shimamoto, K. & Gouaux, E. *Nature* **445**, 387–393 (2007).
6. Reyes, N., Ginter, C. & Boudker, O. *Nature* **462**, 880–885 (2009).
7. Verdon, G. & Boudker, O. *Nat. Struct. Mol. Biol.* **19**, 355–357 (2012).
8. Groeneveld, M. & Slotboom, D.J. *Biochemistry* **49**, 3511–3513 (2010).
9. Groeneveld, M. & Slotboom, D.J. *J. Mol. Biol.* **372**, 565–570 (2007).
10. Bastug, T. *et al. PLoS ONE* **7**, e33058 (2012).
11. Huang, Z. & Tajkhorshid, E. *Biophys. J.* **99**, 1416–1425 (2010).
12. Larsson, H.P. *et al. Proc. Natl. Acad. Sci. USA* **107**, 13912–13917 (2010).
13. Slotboom, D.J., Konings, W.N. & Lolkema, J.S. *J. Biol. Chem.* **276**, 10775–10781 (2001).
14. Seal, R.P., Leighton, B.H. & Amara, S.G. *Neuron* **25**, 695–706 (2000).
15. Bendahan, A., Armon, A., Madani, N., Kavanaugh, M.P. & Kanner, B.I. *J. Biol. Chem.* **275**, 37436–37442 (2000).
16. Zhang, Y., Bendahan, A., Zarbiv, R., Kavanaugh, M.P. & Kanner, B.I. *Proc. Natl. Acad. Sci. USA* **95**, 751–755 (1998).
17. Kavanaugh, M.P., Bendahan, A., Zerangue, N., Zhang, Y. & Kanner, B.I. *J. Biol. Chem.* **272**, 1703–1708 (1997).
18. Rosental, N. & Kanner, B.I. *J. Biol. Chem.* **285**, 21241–21248 (2010).
19. Hänelt, I., Wunnicke, D., Bordignon, E., Steinhoff, H.J. & Slotboom, D.J. *Nat. Struct. Mol. Biol.* **20**, 210–214 (2013).
20. Georgieva, E.R., Borbat, P.P., Ginter, C., Freed, J.H. & Boudker, O. *Nat. Struct. Mol. Biol.* **20**, 215–221 (2013).

ONLINE METHODS

Chemicals. Restriction enzymes and antarctic phosphatase were purchased from New England BioLabs Inc., T4 DNA ligase from Thermo Scientific, L-[^{14}C]aspartate (1.85 MBq, 7.4 GBq/mmol) from PerkinElmer and lipids from Avanti Polar Lipids Inc. L-Arabinose and ampicillin sodium salt were from Sigma-Aldrich. All chemicals were analytical purity grade.

DNA manipulation, protein purification and concentration determination. C-terminally His_8-tagged Glt_{Tk} was purchased from Geneart. Glt_{Tk} was cloned into the pBAD24 vector using standard cloning methods. *Escherichia coli* MC1061 cells containing the plasmid were cultivated in LB medium (37 °C and 200 r.p.m.), and protein was produced by inducing cells at an OD_{600} of 0.8 with 0.05% L-arabinose for 3 h. Harvesting, membrane vesicle preparation, determination of total protein concentration and solubilization in *n*-dodecyl-β-D-maltopyranoside were done as described before[8]. To obtain apo-Glt_{Tk}, we used the procedure that also yielded apo-Glt_{Ph}, with minor modifications as described below[8]. The crucial difference between this purification procedure and the one used by the Gouaux and Boudker labs[4] is the omission of Na^+ from all buffers. In sodium-containing buffers, the substrate aspartate remains associated with the protein throughout the entire purification because the k_{off} is very low. In the absences of sodium ions, the substrate aspartate is lost during the purification. After solubilization, the solution was subjected to ultracentrifugation for 30 min at 4 °C, 265,000*g*. The supernatant was incubated for 1 h on a rotating platform at 4 °C with 0.5 mL bed volume Ni-Sepharose (GE Healthcare) pre-equilibrated with 50 mM Tris HCl, pH 8, 300 mM KCl, 0.15% *n*-decyl-β-D-maltopyranoside (DM), 15 mM imidazole, pH 8. The solution was then loaded onto a Poly-Prep chromatography column (Bio-Rad), which was washed with 20 column volumes (CV) of 50 mM Tris HCl, pH 8, 300 mM KCl, 0.15% DM, 60 mM imidazole, pH 8. Glt_{Tk} was eluted with 50 mM Tris HCl, pH 8, 300 mM KCl, 0.15% DM, 500 mM imidazole, pH 8. The protein was further purified by size exclusion chromatography (SEC) on a Superdex 200 10/300 GL (GE Healthcare) column using 10 mM HEPES-KOH, pH 8, 100 mM KCl, 0.15% DM as running buffer. For crystallization trials the peak fractions were used. After purification, the protein concentration was determined by UV absorption (NanoDrop), using the molecular weight and extinction coefficient calculated by the ExPASy ProtParam tool (web.expasy.org/protparam/). The protein was concentrated to ~7 mg/mL using a spin concentrator (Vivaspin 2, 30,000 MWCO, PES membrane, Vivaproducts).

Crystallization and structure determination. The best diffracting crystals were obtained by the vapor diffusion method in hanging drop with a protein concentration of 7 mg/mL and a reservoir solution of 25% glycerol/polyethylene glycol (PEG) 4000/glycerol, 100 mM Tris/bicine, pH 8.5, 60 mM $CaCl_2$/$MgCl_2$ and 0.5% *n*-octyl-β-D-glucopyranoside (OG). Data sets were collected at ESRF beamlines ID 23-1 and ID 29.

Data processing was performed with XDS with the highest resolution limit of 3.0 Å. The structure was solved with Phaser software using only one monomer of Glt_{Ph} (PDB 2NWX) as a search model. The refinement was done in PHENIX with application of NCS and TLS restraints. To remove bias, several rounds of simulated annealing were performed. Manual correction and building was performed in Coot. Structural figures were generated with PyMOL.

Reconstitution and activity assays. Glt_{Tk} was reconstituted into liposomes consisting of a 3:1:1 mixture of 1,2-dioleoyl-*sn*-glycero-3-phosphoethanolamine (DOPE):1,2-dioleoyl-*sn*-glycero-3-phosphocholine (DOPC):1,2-di-(9*Z*-octadecenoyl)-*sn*-glycero-3-phospho-(1′-*rac*-glycerol) (DOPG) according to Hänelt[19]. Transport assays were performed essentially as described before[8]. All assays were done at 30 °C with stirring, under iso-osmotic conditions. External buffer (50 mM sodium phosphate, pH 6, 7 or 8; or 50 mM Tris/MES, pH 6, 7 or 8), supplemented with 0.23 μM L-[^{14}C]aspartate (PerkinElmer) and 0.6 μM valinomycin was mixed with the proteoliposomes containing 1 μg Glt_{Tk} in a 100:1 (v/v) ratio. For substrate competition experiments a 400-fold excess of unlabeled L-aspartate, D-aspartate or L-glutamate was added to the external buffer. 200-μL samples were taken at each time point, transferred immediately into 2 mL ice-cold outside buffer and filtered over a 0.45-μm-pore-size filter (Protran Ba 85, Whatman). The filters were transferred to a 2-mL reaction tube, 2 mL scintillation liquid (Emulsifier Scintillator Plus, PerkinElmer) was added and the filters were allowed to dissolve. All samples were measured in a PerkinElmer Tri-Carb 2800RT liquid scintillation counter.

ITC. ITC experiments were performed at a constant temperature of 25 °C using an ITC200 calorimeter (MicroCal). The thermally equilibrated ITC cell was filled with 200 μl of purified Glt_{Tk} (concentration 13–15 μM, in 10 mM HEPES/KOH, pH 8, 100 mM KCl, 0.15% DM with or without 500 mM NaCl). 100 μM aspartate (dissolved in the same buffer as the protein) was titrated into the cell in steps of 2 μL. Data was analyzed using the software provided by MicroCal.